

Article

Substrate recognition and specificity of double-stranded RNA binding proteins

Lela Vukovic, Hye Ran Koh, Sua Myong, and Klaus Schulten

Biochemistry, **Just Accepted Manuscript** • DOI: 10.1021/bi500352s • Publication Date (Web): 06 May 2014

Downloaded from <http://pubs.acs.org> on May 12, 2014

Just Accepted

“Just Accepted” manuscripts have been peer-reviewed and accepted for publication. They are posted online prior to technical editing, formatting for publication and author proofing. The American Chemical Society provides “Just Accepted” as a free service to the research community to expedite the dissemination of scientific material as soon as possible after acceptance. “Just Accepted” manuscripts appear in full in PDF format accompanied by an HTML abstract. “Just Accepted” manuscripts have been fully peer reviewed, but should not be considered the official version of record. They are accessible to all readers and citable by the Digital Object Identifier (DOI®). “Just Accepted” is an optional service offered to authors. Therefore, the “Just Accepted” Web site may not include all articles that will be published in the journal. After a manuscript is technically edited and formatted, it will be removed from the “Just Accepted” Web site and published as an ASAP article. Note that technical editing may introduce minor changes to the manuscript text and/or graphics which could affect content, and all legal disclaimers and ethical guidelines that apply to the journal pertain. ACS cannot be held responsible for errors or consequences arising from the use of information contained in these “Just Accepted” manuscripts.



Substrate recognition and specificity of double-stranded RNA binding proteins

Lela Vuković^{1,2}, Hye Ran Koh^{1,2}, Sua Myong^{2,3}, and Klaus Schulten^{1,2}

¹*Department of Physics, University of Illinois at Urbana-Champaign, Urbana, IL 61801, United States*

²*Center for the Physics of Living Cells, University of Illinois at Urbana-Champaign, Urbana, IL 61801, United States and*

³*Department of Bioengineering, University of Illinois at Urbana-Champaign, Urbana, IL 61801, United States*

(Dated: April 30, 2014)

Abstract

Recognition of double-stranded (ds) RNA is an important part of many cellular pathways, including RNA silencing, viral recognition, RNA editing, processing and transport. dsRNA recognition is often achieved by dsRNA binding domains (dsRBDs). We use atomistic molecular dynamics simulations to examine the binding interface of the transactivation response RNA binding protein (TRBP) dsRBDs to dsRNA substrates. Our results explain the exclusive selectivity of dsRBDs towards dsRNA and against DNA-RNA hybrid and dsDNA duplexes. We also provide corresponding experimental evidence. The dsRNA duplex is recognized by dsRBDs through the A-form of three duplex grooves and by the chemical properties of RNA bases, which have 2'-hydroxyl groups on their sugar rings. Our simulations show that TRBP dsRBD discriminates dsRNA from DNA-containing duplexes primarily through interactions at two duplex grooves. The simulations also reveal that the conformation of the DNA-RNA duplex can be modulated by dsRBD proteins, suggesting a potentially weak binding of dsRBDs to DNA-RNA hybrids. Our study reveals the structural and molecular basis of protein-RNA contact that gives rise to the substrate specificity of dsRNA binding proteins.

E-mail: smyong@illinois.edu, lvukov1@illinois.edu, kschulte@ks.uiuc.edu

Funding: National Science Foundation (grant NSF-PHY-0822613) and National Institutes of Health (grant NIH 9P41GM104601).

1 ABBREVIATIONS

2
3
4 dsRNA, double-stranded RNA; dsRBD, dsRNA binding domain; TRBP, transactivation
5 response RNA binding protein; PKR, protein kinase R; RHA, RNA helicase A; mRNA,
6 messenger RNA; ADAR, adenosine deaminase acting on RNA; PACT, protein activator
7 of PKR; MD, molecular dynamics; EMSA, electrophoretic mobility shift assay; bp, base
8 pair; TRBP-RBD2, second dsRBD of TRBP; PME, particle-mesh Ewald; SASA, solvent
9 accessible surface area; TRBP-RBD1, first dsRBD of TRBP.
10
11
12
13
14
15
16
17
18
19
20
21
22
23
24
25
26
27
28
29
30
31
32
33
34
35
36
37
38
39
40
41
42
43
44
45
46
47
48
49
50
51
52
53
54
55
56
57
58
59
60

1. Introduction

RNA is emerging as an important regulatory element of many cellular processes [1–4]. Double stranded (ds) RNA is a frequent structural element of the cellular RNA; accordingly, cells synthesize many proteins which recognize it. dsRNA binding domain (dsRBD) is one of the most abundant RNA binding domains [5, 6], found in proteins localized both in cell nuclei and cytoplasm [7]. dsRBD proteins primarily regulate gene expression and signaling events. For example, the protein kinase PKR binds viral dsRNA and signals the onset of infection [8]; RNA helicase A (RHA) unwinds dsRNA [9]; the Dicer enzyme binds to and slices dsRNA into 21-22 nucleotide long pieces, which silence mRNA [10, 11]; adenosine deaminase acting on RNA (ADAR) edits adenosine bases of dsRNA and converts them to inosines [12]. Many dsRBD proteins contain multiple dsRBDs. For example, two dsRBDs are found in RHA, three dsRBDs are found in ADAR1, in protein activator of PKR (PACT) and in transactivation response RNA binding protein (TRBP), and five dsRBDs are found in Staufen [7].

TRBP participates in multiple cellular pathways in cell nuclei and cytoplasm [13]. In gene silencing by the RNA interference pathway, TRBP, Dicer, and PACT proteins are essential components of the RNA-induced silencing complex [14–17]. Biochemical and cryo-electron microscopy experiments have shown that two of TRBP dsRBDs aid in positioning of dsRNA in the proper conformation for dsRNA cutting by Dicer [18]. In our recent single molecule experiments we found that TRBP and Dicer-TRBP bind to and diffuse on dsRNA duplexes [19]. Interestingly, TRBP does not bind to other duplex types, including dsDNA and even DNA-RNA hybrids [19, 20]. Many other dsRBD proteins specifically bind to dsRNA duplexes, while some also weakly bind to DNA-RNA hybrid duplexes [21, 22].

Considering the above experimental data about dsRBD binding targets, there are two questions of particular interest: (1) How do dsRBDs discriminate between nucleic acid duplexes of similar structures, such as dsRNA, DNA-RNA, and dsDNA; (2) How do dsRBDs discriminate between dsRNA of different sequences, abundant in the cell nuclei and cytoplasm? In the present study, we address the first question. Currently, the mechanism of dsRBD discrimination of dsRNA, DNA-RNA, and dsDNA has been explored only through static (crystal) structures of several different dsRBDs to short pieces of dsRNA [5] and short (2 ns) simulations [23]. Here, we examine by experiments and atomistic molecular

1 dynamics (MD) simulations the binding of TRBP dsRBDs to dsRNA, DNA-RNA and ds-
2 DNA duplexes. Our simulations identify the molecular mechanism of dsRNA recognition by
3 dsRBDs; in particular, they reveal why dsRBDs bind weakly to DNA-RNA duplexes, but
4 do not bind to dsDNA duplexes.
5
6
7

8 2. Methods.

9
10 *Electrophoretic mobility shift assay.* In order to experimentally investigate binding
11 of TRBP-RBD2 to dsRNA, DNA-RNA, and dsDNA, we performed an electrophoretic
12 mobility shift assay (EMSA). We prepared three types of 25-bp duplexes with the
13 same sequence (*forward*: 5'-GCUUGUCGGGAGCGCCACCCUCUGC-3', *reverse*: 5'-
14 GCAGAGGGUGGCGCUCCCGACAAGC-3'; T instead of U for DNA strands), which were
15 labeled with either DY547 or Cy3 at the 3' end of the reverse strand. We incubated 10 nM of
16 25-bp duplexes with various concentrations of TRBP-RBD2 ranging from 1 μ M up to 10 μ M
17 in binding buffer (20 mM Tris-HCl, pH 7.5, 25 mM NaCl, 1 mM DTT, and 0.1 mg/ml BSA)
18 on the ice for 20 min. Then, 8 μ l of the incubated sample was mixed with 2 μ l of RNA
19 loading dye (NEB) and loaded immediately in the 6 % DNA retardation gel (Invitrogen).
20 We took the fluorescence gel images after running the gel at 100 V for 40 min and analyzed
21 the band density with Image J (<http://rsbweb.nih.gov/ij/>).
22
23
24
25
26
27
28
29
30
31

32 *Atomic resolution models.* To examine mechanisms of dsRNA recognition by dsRBD
33 domains, we simulated three complexes: (i) TRBP-RBD2 : dsRNA, (ii) TRBP-RBD2 :
34 DNA-RNA, and (iii) TRBP-RBD2 : dsDNA, where TRBP-RBD2 labels the second dsRBD
35 of TRBP. TRBP-RBD1 : dsRNA complex and dsRNA, DNA-RNA and dsDNA duplexes
36 were simulated also separately for comparison. The initial structures of complexes (i-iii) were
37 based on the crystal structure of TRBP-RBD2 bound to coaxially stacked RNA duplexes
38 (Protein Data Bank entry code 3ADL) [24]. The initial structures of dsRNA, DNA, and
39 DNA-RNA duplexes, 35-base pairs in length, were generated in their A-forms by the 3DNA
40 software [25]. The simulated dsRNA duplexes contained complementary strands, where the
41 5'→3' strand had the sequence UAACAACCAGAUCAAAGAAAAACAGACAUUGUCA,
42 as in our previous experiments [19]. DNA strands had sequences analogous to RNA strands,
43 with the exception that U bases were replaced with T bases. In the initial structures of
44 complexes, TRBP-RBD2 was positioned approximately in the middle of the duplexes in
45 order to avoid its interaction with duplex edges, as shown in Fig. 1.
46
47
48
49
50
51
52
53
54
55

56 The *cionize* code was used to place Na⁺ counterions neutralizing nucleic acid charges
57
58
59
60

1 around the prepared duplexes and complexes. The resulting structures were solvated in
2 TIP3P water and 50 mM NaCl with *solvate* and *ionize* VMD plugins [26]. The final sys-
3 tems contained approximately 80,000 atoms (in case of simulations involving duplexes) and
4 105,000 atoms (in case of simulations involving proteins and duplexes).
5
6
7

8 *Molecular Dynamics Simulations.* MD simulations were performed with NAMD2 software
9 [27], where the systems were described assuming the AMBER force field with SB [28] and
10 BSC0 [29] corrections, a suitable choice for describing RNA [30, 31]. The particle-mesh
11 Ewald (PME) method [32] was used for evaluation of long-range Coulomb interactions. The
12 timestep was set to 1.0 fs, and long range interactions were evaluated every 2 (van der Waals)
13 and 4 timesteps (Coulombic). After 2,000 steps of minimization, ions and water molecules
14 were equilibrated for 2 ns around duplexes and complexes, which were constrained using
15 harmonic forces with a spring constant of 1 kcal/molÅ². Then, unconstrained duplexes and
16 complexes were simulated for 50 ns and 100 ns, respectively. The simulations were performed
17 in NpT ensemble, at a constant temperature T= 310 K, a Langevin constant $\gamma_{Lang} = 1.0$
18 ps⁻¹, and at a constant pressure p= 1 bar.
19
20
21
22
23
24
25
26
27

28 *Data analysis.* To analyze the binding of TRBP-RBD2 to three duplexes, we computed
29 the contact area a_{con} in dependence on time t , defined as:
30
31

$$32 \quad a_{con}(t) = \frac{a_{dsRBD}(t) + a_{dupl}(t) - a_{dsRBD:dupl}(t)}{2}, \quad (1)$$

33
34

35 where a_{dsRBD} , a_{dupl} and $a_{dsRBD:dupl}$ are the solvent accessible surface areas (SASA) of TRBP-
36 RBD2, nucleic acid duplex and TRBP-RBD2:duplex complex, respectively. The evaluation
37 was done by the SASA built-in VMD plugin [26], where the van der Waals radius of 1.4 Å was
38 assigned to atoms to identify the points on a sphere that are accessible to the solvent. We
39 also calculated the interaction energy between TRBP-RBD2 and each nucleic acid duplex
40 by the NAMDenergy function in VMD [26].
41
42
43
44
45

46 The forms of duplexes were analyzed from single averaged structures of duplexes and
47 complexes. These averaged structures were obtained by averaging the coordinates of aligned
48 duplexes and complexes over specified portions of trajectories. The helical rise values for
49 nucleic acid duplexes, which characterize duplex forms, were evaluated with the 3DNA
50 software [25].
51
52
53
54
55

56 3. Results.

57
58
59
60

1 The fact that TRBP protein recognizes dsRNA over DNA-RNA and dsDNA has been
2 established in previous experiments [19–21, 33]. Here we examine through MD simulations
3 and experiment how TRBP dsRBDs recognize dsRNA duplexes over nucleic acid duplexes
4 that contain DNA.
5
6
7

8 **TRBP-RBD2 binding to nucleic acid duplexes in EMSA gels.** In order to examine
9 relative binding affinities of TRBP-RBD2 for dsRNA, DNA-RNA and dsDNA duplexes,
10 we performed electrophoretic mobility shift assays (EMSA) for solutions containing these
11 duplexes and 0, 1 μM , 3 μM or 10 μM TRBP-RBD2. The resulting EMSA gels, shown in
12 Fig. 2, contain strong upper bands in lines 2 and 3, indicating that TRBP-RBD2 : dsRNA
13 complexes are formed at 1 μM , 3 μM and 10 μM TRBP-RBD2 concentrations. The fact that
14 in Fig. 2 (b) the location of the upper band in line 3 is higher than in line 2 indicates that the
15 number of bound TRBP-RBD2 molecules per dsRNA duplex increases with TRBP-RBD2
16 concentration. There is usually no relative affinity of dsRBDs for DNA-RNA and dsDNA
17 reported in the literature [19–21]. Here, the EMSA gel in Fig. 2 (b) shows that 10 μM
18 TRBP-RBD2 binds to DNA-RNA and does not bind to dsDNA. Therefore, TRBP-RBD2
19 has the greatest affinity for dsRNA, a smaller affinity for DNA-RNA, and no affinity for
20 dsDNA at the tested TRBP-RBD2 concentrations.
21
22
23
24
25
26
27
28
29
30

31 **TRBP-RBD2 binding to dsRNA in MD simulations.** In Fig. 1 (a,b), we show
32 a snapshot of TRBP-RBD2 in complex with a 35-base pair RNA duplex, based on the
33 crystal structure of TRBP-RBD2 with coaxially stacked RNA duplexes [24]. TRBP-RBD2, a
34 domain with the $\alpha\beta\beta\beta\alpha$ fold, binds to dsRNA along the duplex axis and across three grooves
35 of the duplex (minor-major-minor grooves), similar to other dsRBDs [34–37]. dsRNA minor
36 grooves are lined with 2'-hydroxyl groups on sugar rings of RNA nucleotides, and the major
37 grooves are lined with the negatively charged phosphate ($-\text{PO}_4^-$) groups. dsRNA duplex
38 assumes A-form, in which the widths of minor and major grooves are comparable (Fig. 1
39 (a)).
40
41
42
43
44
45
46
47

48 The contacts between TRBP-RBD2 and dsRNA are either direct (hydrogen bonding)
49 or water-mediated (hydrogen bonding through water molecules that have long residence
50 times). Bases of the minor groove I contact polar (His159, Gln165) and negatively charged
51 (Glu166) residues, and bases of the minor groove II contact polar (His188) and positively
52 charged (Arg189, Lys190) residues (Fig. 1 (b)). The $-\text{PO}_4^-$ groups of the dsRNA major
53 groove contact polar (Thr208) and positively charged (Lys210, Lys211, Lys214, Arg215)
54
55
56
57
58
59
60

1 residues of helix α_2 , which lies across the width of the major groove.

2
3 In Fig. 1 (c), we compare the sequences of two RBDs in TRBP. Interestingly, not all the
4 residues, which contribute to binding of TRBP-RBD2 to dsRNA, are conserved: Glu166,
5 His188, Lys210, Lys211, and Lys214 are conserved, while Gln165, Arg189, Lys190, and
6 Arg215 are not conserved.
7
8
9

10 **TRBP-RBD2 binding to non-cognate substrates.** Next, we examine the binding
11 of TRBP-RBD2 to nucleic acid duplexes containing DNA. Snapshots of TRBP-RBD2 in
12 complex with DNA-RNA and dsDNA, captured at the end of 100 ns long simulations, are
13 shown in Fig. 3 (a,b), respectively. For comparison, the TRBP-RBD2 : dsRNA complex is
14 overlaid as a shadow. Even though the simulations were started with DNA-RNA and dsDNA
15 duplexes in A-forms, these duplexes changed to B-forms within several nanoseconds of the
16 simulations; in MD simulations with the selected force field [29], free dsDNA duplexes assume
17 B-forms [38] and free dsRNA duplexes assume A-forms [30], in agreement with experimental
18 data. Quick (≈ 1 ns) A \rightarrow B form changes of DNA strands in dsDNA and DNA:RNA duplexes
19 were observed and characterized in previous short scale simulations [39]. After 100 ns of
20 equilibration, DNA-RNA and dsDNA duplexes are significantly longer than dsRNA, despite
21 all duplexes having the same number of base pairs. During simulations, DNA-RNA and
22 dsDNA relaxed to forms with significantly wider major grooves and narrower minor grooves,
23 thus departing from their initial A-forms. Analyses of selected helical parameters (Table S1),
24 including twist, slide, and roll, show that DNA-RNA and dsDNA duplexes in complex with
25 TRBP-RBD2 have distinct non-A-forms, and are similar in form to free duplexes [39, 40].
26 In addition, Table S1 shows that DNA strands of DNA-RNA and dsDNA duplexes acquire
27 dihedral angles (δ , ϵ) and phase angles of pseudorotation (P) characteristic of DNA strands
28 in B-form, comparable to values reported in [40].
29
30
31
32
33
34
35
36
37
38
39
40
41
42
43

44 Results in Figs. 1 (b) and 3 show that DNA-RNA and dsDNA duplexes stay in contact
45 with a smaller number of TRBP-RBD2 residues than does dsRNA. Binding of TRBP-RBD2
46 to minor groove I is significant only for the dsRNA duplex, where helix α_1 lies across the
47 minor groove I and remains in close contact with it. Minor grooves I of DNA-RNA and
48 dsDNA are more exposed to solvent, since helix α_1 is lifted from the groove. Binding of
49 TRBP-RBD2 to major grooves is also more prominent for dsRNA. The number of TRBP-
50 RBD2 contacts to the minor groove II is very similar in case of all three studied duplexes.
51
52
53
54
55

56 Figs. 4 (a) and (c) show contact areas and interaction energies of TRBP-RBD2 and three
57
58
59
60

1 duplexes, evaluated during the last 85 ns of the simulations. The contact area decreases
2 (Fig. 4 (a)) and binding energy becomes less favorable (Figs. 4 (c)) as the DNA content of the
3 duplex increases. The number of hydrogen bonds between TRBP-RBD2 and three duplexes
4 also decreases with the increase of DNA content (Fig. S3), confirming that TRBP-RBD2
5 binds most favorably to its cognate substrate, dsRNA, in agreement with our experiments.
6
7
8
9

10 The individual contributions to the net contact area are shown for each (minor-major-
11 minor) groove in Fig. 4 (b). These contact areas were evaluated between whole duplexes
12 and selected groups of TRBP-RBD2 amino acid residues directly above each of the grooves.
13 The results confirm that TRBP-RBD2 has much less contact with the minor groove I in case
14 of DNA-containing duplexes than in case of the dsRNA duplex; the contact area between
15 TRBP-RBD2 and DNA-RNA or dsDNA minor grooves I is only $\approx 40 - 50\%$ of the contact
16 area between TRBP-RBD2 and dsRNA minor groove I. The contact area between TRBP-
17 RBD2 and the duplex major groove also decreases with the increased DNA content of the
18 duplex. The results indicate that TRBP-RBD2 recognizes dsRNA based on interactions in
19 minor groove I and in the major groove.
20
21
22
23
24
25
26
27

28 **TRBP-RBD2 recognizes dsRNA over DNA-containing substrates.**

29 *Recognition at the major groove.* The binding mode of TRBP-RBD2 to the major
30 groove of dsRNA is shown in Fig. 5 (a). Five amino acid residues, Thr208, Lys210, Lys211,
31 Lys214, and Arg215, make direct contact to the dsRNA backbone at the major groove.
32 Thr208, Lys210, Lys214, and Arg215 bind to the parts of the dsRNA major groove directly
33 beneath them. On the other hand, Lys211 lies across the major groove. Its backbone atoms
34 are on one side of the groove, while its positively charged tip contacts the $-\text{PO}_4^-$ group on
35 the opposite side of the major groove.
36
37
38
39
40
41
42

43 The stability of binding between the five identified residues to major grooves of dsRNA,
44 DNA-RNA and dsDNA is examined by tracking distances of these residues to their nearest
45 neighbor $-\text{PO}_4^-$ groups. In Fig. 5 (b), we show these distances averaged over the last 85
46 ns of trajectories (time evolution of these distances is shown in Fig. S4). The results show
47 that Thr208 makes a hydrogen bond to the nearest $-\text{PO}_4^-$ group in dsRNA and DNA-
48 RNA duplexes, but does not engage in hydrogen bonding in case of the dsDNA duplex.
49 The distances between Lys210 and Arg215 to the nearest $-\text{PO}_4^-$ groups are similar for all
50 three duplexes, but the distances between Lys211 and Lys214 to the nearest $-\text{PO}_4^-$ groups
51
52
53
54
55
56
57
58
59
60

1 are perturbed when the duplex contains DNA, involving a gradual increase in the average
2 distance of Lys211 to the nearest $-\text{PO}_4^-$ group with the increase of DNA content in the
3 duplex. Likewise, the distance between Lys214 to the nearest $-\text{PO}_4^-$ group becomes longer
4 and less stable for DNA-containing duplexes.
5
6
7

8 While the results in Fig. 5 (b) show that Lys211 and Lys214 enable TRBP-RBD2 to
9 recognize and bind to dsRNA, experiments have shown that single mutations of His188,
10 Lys210 and Lys214 block TRBP-RBD2 binding to dsRNA [13]. A closer look at the binding
11 mode of TRBP-RBD2 and the dsRNA major groove indicates that Lys210 and Lys214
12 form a pair that bridges $-\text{PO}_4^-$ groups on two sides of the dsRNA major groove. In Fig. 5
13 (c-e), we analyze the distances between Lys210 and Lys214, and between $-\text{PO}_4^-$ groups
14 which coordinate them (the distances are measured between the nitrogen atoms of Lys210
15 and Lys214 sidechains, and between the phosphate atoms of RNA nucleotides 17 and 48,
16 respectively). The results show evidence for a “register” fit of Lys210-Lys214, as the lysine
17 pair fits exactly above the $-\text{PO}_4^-$ groups which coordinate them. The distance between
18 positively charged tips of Lys210 and Lys214 residues is always in the range $\approx 9 - 13 \text{ \AA}$,
19 while the distance between the bridging $-\text{PO}_4^-$ groups increases from $\approx 11 \text{ \AA}$ for dsRNA to
20 $\approx 17 \text{ \AA}$ for DNA-RNA and to $\approx 20 \text{ \AA}$ for dsDNA. Therefore, the Lys210-Lys214 pair fits
21 poorly in the major grooves of DNA-RNA and dsDNA duplexes because the major grooves
22 of these duplexes are significantly wider, as shown in Fig. S5. Similarly, Lys211 cannot
23 effectively bridge the $17 - 20 \text{ \AA}$ distance across the major groove of DNA-RNA and dsDNA.
24
25
26
27
28
29
30
31
32
33
34
35
36
37 **Recognition at minor grooves.** dsRBDs bind to two minor grooves of dsRNA [24, 34–
38 37], in the binding mode shown in Fig. 1 (a). Minor grooves of dsRNA are lined with
39 2'-hydroxyl (OH) groups, located on the sugar rings of RNA bases. However, DNA bases
40 lack 2'-hydroxyl groups. To explore the effect of the 2'-OH groups on dsRBD binding to
41 three duplexes, we analyze the dsRBD binding to minor grooves I and II.
42
43
44
45

46 Snapshots of TRBP-RBD2 bound to minor grooves I of dsRNA and dsDNA are shown
47 in Fig. 6 (a,b). When TRBP-RBD2 binds to dsRNA, its α_1 -helix extends across the groove.
48 His159 and Gln165 residues of the α_1 -helix make three direct hydrogen bonds to dsRNA, and
49 Glu166 makes one water-mediated bond. The three direct hydrogen bonds remain stable for
50 most of the time during the last 85 ns of the trajectory, whereas the water-mediated bond
51 exhibits significant fluctuation (Fig. 6 (c)). On the other hand, TRBP-RBD2 does not bind
52 across the minor groove I of dsDNA. Figure 6 (b,d) shows that for this complex only Gln165
53
54
55
56
57
58
59
60

1 makes a hydrogen bond to the phosphate group of the nearest DNA nucleotide, albeit only
2 a fluctuating one. Binding of TRBP-RBD2 to DNA-RNA is very similar to its binding to
3 dsDNA (not shown).
4
5

6 Fig. 6 (a,b) demonstrates that minor grooves I of dsRNA and dsDNA have different
7 forms: the minor groove I of dsRNA is wide and shallow (A-form like), with its bases being
8 in contact with TRBP-RBD2 helix α_1 , whereas minor groove I of dsDNA is narrower and
9 much deeper (B-form like), with its bases being buried below the α_1 helix. The results in
10 Fig. 6 show clearly that the A-form of the minor groove I facilitates TRBP-RBD2 binding.
11
12
13

14 TRBP-RBD2 exhibits a binding (contact) area to minor groove II that is similar for all
15 three duplexes (Fig. 4 (b)). However, the binding modes in this groove differ between the
16 three duplexes. For TRBP-RBD2 bound to dsRNA minor groove II, the His188 hydrogen
17 binds to the 2'-OH group, while Arg189 and Lys190 occasionally interact with the 2'-OH
18 groups or the backbone phosphate groups. For TRBP-RBD2 bound to DNA-RNA minor
19 groove II, His188 is unbound, while Arg189 and Lys190 form stable hydrogen bonds to two
20 bases. Lastly, for TRBP-RBD2 bound to dsDNA, His188 makes a hydrogen bond to one of
21 the bases, while Arg189 and Lys190 bind Coulombically to the negatively charged backbone
22 phosphate groups. Since Arg189 and Lys190 residues are not conserved, dsRBDs without
23 these residues would exhibit weaker binding to the minor groove II of DNA-containing
24 duplexes.
25
26
27
28
29
30
31
32
33
34

35 ***Duplex form at TRBP-RBD2 binding site.*** Results in Figs. 5 and 7 already show
36 that the duplex form with its minor and major grooves plays a significant role in optimal
37 TRBP-RBD2 binding. Here, we examine the complete duplex forms at the sites of binding
38 to TRBP-RBD2. To compare in this regard the dsRNA, DNA-RNA, and dsDNA duplex
39 forms at TRBP-RBD2 binding sites, single average structures of the respective complexes
40 were characterized by considering structures averaged over the last 40 ns of trajectories and
41 then aligning the TRBP-RBD2 domains of these structures.
42
43
44
45
46
47

48 The resulting duplexes at the binding site are shown in Fig. 7 (a). Several structural
49 features can be clearly discerned. First, the width of the major groove is narrowest for
50 dsRNA, wider for DNA-RNA and widest for dsDNA. The increase in the major groove
51 width with the increased DNA content is the reason for the gradual decrease of TRBP-
52 RBD2 binding to the major groove of the three duplexes (Fig. 4 (b)). Second, minor grooves
53 I of DNA-RNA and dsDNA can be almost perfectly superimposed on each other, but not
54
55
56
57
58
59
60

1 to the more compressed minor groove I of dsRNA; only dsRNA achieves stable binding to
2 TRBP-RBD2. Third, at the minor groove II DNA-RNA assume almost identical forms as
3 dsRNA, whereas dsDNA exhibits a much narrower minor groove II.
4

5
6 When DNA-RNA is simulated without bound TRBP-RBD2, both of its minor grooves
7 resemble closely the dsDNA minor grooves (Fig. S6 (b)). Therefore, through the presence
8 of TRBP-RBD2, the minor grooves of DNA-RNA adopt either dsRNA or dsDNA forms,
9 depending on the interactions with the protein (Fig. S5 (b)). Similar duplex flexibility and
10 duplex adaptation to bound proteins has been observed for dsDNA duplexes [41]. Interest-
11 ingly, it is the DNA strand of the DNA-RNA minor groove II that changes its conformation
12 and is almost perfectly overlaid with the RNA strand of the dsRNA, as shown in Fig. 7 (a).
13
14

15
16 In Fig. 7 (b), we compare the helical rise of the duplexes simulated with bound TRBP-
17 RBD2. The helical rise is the distance between neighboring bases in the duplex helix. For
18 perfect A-form dsRNA it is ≈ 2.5 Å, whereas for B-form dsDNA it is 3.4 Å. For duplexes
19 bound to TRBP-RBD2, the helical rise is evaluated for the averaged structures. The results
20 show for dsRNA a perfect A-form, except in one region of widened major groove (exper-
21 imentally confirmed for dsRBDs [34]). For DNA-RNA, the helical rise is between A- and
22 B-forms, as observed in other studies of free DNA-RNA duplexes [39, 40]; for dsDNA the
23 helical rise is again between A- and B-form, but very close to the B-form value. dsRNA has
24 the smallest helical rise and remains closest to the A-form.
25
26

27
28 In Table S1, we further quantify forms of duplexes bound to TRBP-RBD2 and list their
29 selected average helical parameters (twist, slide, roll), as well as dihedral angles (δ , ϵ) and
30 phase angles of pseudorotation (P). Comparison of Table S1 to parameters of free duplexes
31 [40] shows that free and dsRBD-bound duplexes have similar forms. Overall, DNA strands
32 in dsDNA and DNA-RNA duplexes have parameters characteristic of B-form, whereas RNA
33 strands in dsRNA and DNA-RNA have parameters characteristic of A-form. However,
34 dihedral angles δ and phase angles P of DNA nucleotides in TRBP-RBD2 : DNA-RNA
35 complex, shown in Fig. S8, show that DNA nucleotides can switch to A-form when bound
36 to TRBP-RBD2.
37
38

39 4. Discussion.

40
41 In the present article, we have clarified by means of MD simulations the experimen-
42 tal observation that dsRBDs recognize and bind to dsRNA, and avoid binding to simi-
43
44
45
46
47
48
49
50
51

1 lar DNA-RNA and dsDNA duplexes. Previous experiments showed that isolated first and
2 second dsRBDs of TRBP bind stably to dsRNA, with binding affinities of 220 nM and
3 110 nM, respectively [42]. Our experiments, shown in Fig. 2, confirmed that TRBP-RBD2
4 (1-10 μ M) binds to dsRNA. In agreement with experiments, MD simulations showed that
5 TRBP dsRBDs bind stably to dsRNA, with the second dsRBD having a more favorable
6 interaction energy with dsRNA than the first dsRBD (Fig. S9).
7
8
9

10 While there are examples of domains and proteins that can bind to both RNA and DNA
11 [43–46], TRBP and other dsRBD-containing proteins do not bind well to DNA-RNA and
12 dsDNA duplexes [19–21]. For example, dsRBDs of PKR bind to dsRNA and DNA-RNA
13 with $K_d = 0.17 \mu\text{M}$ and $\geq 500 \mu\text{M}$, respectively, while no binding to dsDNA was observed in
14 the tested experimental conditions [21]. Whole TRBP protein (10 nM - 2 μ M concentration)
15 binds to dsRNA, but not to DNA-RNA and dsDNA [19, 20]. However, some dsRBD proteins,
16 such as 4F protein that contains two dsRBDs, can bind strongly to both dsRNA and DNA-
17 RNA duplexes; DNA-RNA duplexes at 50 pM concentration were able to compete with
18 dsRNA duplexes for binding to 4F [22]. Our experimental results in Fig. 2 show that at
19 the concentration of 5-10 μ M, TRBP-RBD2 binds to 20-90% of the present DNA-RNA,
20 and does not bind to dsDNA. Therefore, TRBP-RBD2 can discriminate between dsRNA
21 and DNA-RNA more effectively than 4F and less effectively than PKR. In agreement with
22 the experimental results, complexes of TRBP-RBD2 with DNA-RNA and dsDNA were less
23 stable in the performed MD simulations than complexes with dsRNA, as shown in Figs. 1,
24 3, and 4.
25
26
27
28
29
30
31
32
33
34
35
36
37
38

39 MD simulations reveal that the duplex form plays an important role in the recognition of
40 dsRNA over DNA-containing duplexes by dsRBDs, as has already been hypothesized on the
41 basis of dsRBD:dsRNA complex structures [5]. A proper binding of a dsRBD to a nucleic
42 acid duplex is determined by a proper “register fit” of the dsRBD into three successive duplex
43 grooves, which is in turn largely determined by the duplex form. While dsRNA duplex has
44 the A-form, DNA-containing duplexes quickly adopt an intermediate form (DNA-RNA) and
45 the B-form (dsDNA), as seen in Figs. 7 and S6. By adopting B-like forms, DNA-containing
46 duplexes have wider major grooves and narrower minor grooves than dsRNA. For example,
47 the major grooves of DNA-containing duplexes become 6 – 9 Å wider than the major groove
48 of dsRNA (Fig. 5 (c-e)).
49
50
51
52
53
54
55
56

57 As a result of changed forms, binding of TRBP-RBD2 to DNA-RNA and dsDNA becomes
58
59
60

1 significantly impaired in major grooves and in minor grooves I, but not in the minor groove
2 II, as quantified in Fig. 4 (b). Delayed changes of the dsDNA major groove width at the
3 binding site, seen in Fig 5 (e), show the importance of the duplex form for dsRBD binding.
4 Preserved contacts between the dsDNA major groove and three basic residues, Lys 210, Lys
5 211, and Lys 214, keep dsDNA from adopting its preferred major groove width during the
6 first 50 ns of simulations. In comparison, dsDNA without the bound dsRBD adopts very
7 quickly wide major grooves of the B-form. Similarly, TRBP-RBD2 easily contacts the bases
8 in the wide and shallow minor groove I of dsRNA, but cannot contact the bases in the deeper
9 and narrower minor groove I of dsDNA (Fig. 6). In principle, dsRBDs could bind dsDNA if
10 dsDNA was flexible enough to adopt the A-form. However, while B-form DNA was shown
11 to be highly flexible, its distortions do not necessarily change its global helical conformation
12 [47]. Otherwise, dsRBDs could bind DNA-containing duplexes if dsRBDs were flexible and
13 able to structurally conform to these duplexes. However, the simulations show that dsRBDs
14 resist structural changes in the presence of dsDNA and DNA-RNA, and validate previous
15 hypotheses and observations on dsRBD rigidity [5].

16 The contribution of 2'-OH groups to binding of dsRBDs to dsRNA was previously ex-
17 amined for PKR, a protein with two dsRBDs, binding to chimeric dsRNA duplexes with
18 several 2'-OH groups substituted to 2'-H or 2'-OCH₃ [21]. Several results indicated that
19 2'-OH groups play a more important role than duplex form in PKR binding to dsRNA.
20 For example, only one ionic contact was found between PKR and dsRNA, and the muta-
21 genesis studies showed that one Lys residue is required for PKR : dsRNA binding (Lys 60
22 in PKR-RBD1, analogous to Lys 210 in TRBP-RBD2) [48]. However, more recently, crys-
23 tal structures of dsRBD : dsRNA complexes identified multiple ionic interactions between
24 dsRBDs and dsRNA phosphate groups [24, 34]. Mutagenesis studies of TRBP showed that
25 three residues of TRBP-RBD2, His 188, Lys 210, and Lys 214, are required for TRBP-RBD2
26 binding to dsRNA [13]. Smaller involvement of ionic interactions between PKR and dsRNA
27 could be due to PKR lacking several basic residues that contribute to strong binding of
28 TRBP-RBD2 to dsRNA and its major groove. PKR-RBD1 lacks the residues analogous to
29 Arg 190 and Arg 215 of TRBP-RBD2, while PKR-RBD2 lacks the residues analogous to
30 Arg 190, Lys 191, Lys 211, and Arg 215 of TRBP-RBD2 [5]. The observation that the Lys
31 210 and Lys 214 pair of TRBP-RBD2 has to fit well into the major groove of the duplex in
32 order for the dsRBD to bind stably to the duplex, as shown in Fig. 5 (c-e), highlights the
33

1 importance of shape on binding of dsRBDs to duplexes.

2
3 While dsRBDs are known to not bind to DNA-RNA and dsDNA [19–21], experimental
4 results in Figs. 2 and S2 show that TRBP-RBD2 at concentration $> 5 \mu\text{M}$ has a higher
5 binding affinity for DNA-RNA than for dsDNA. The higher affinity of TRBP-RBD2 for
6 DNA-RNA is likely due to the narrower major groove of DNA-RNA (Fig. 5 (d)) and the
7 fact that TRBP-RBD2 can alter the width of DNA-RNA grooves and strengthen the bind-
8 ing. The latter was observed in the minor groove II of the DNA-RNA duplex, which acquired
9 the width of an A-form duplex, due to DNA nucleotides changing from B to A-form con-
10 formations (Fig. S8) upon binding to TRBP-RBD2 (Fig. S7 (b)). The observed B→A-form
11 change of DNA nucleotides and the resulting minor groove width modulation potentially
12 explain how other dsRBD proteins, such as 4F [22], can also bind to DNA-RNA hybrids.

13
14 In the present article we have shown how dsRNA binding proteins distinguish between
15 dsRNA and DNA-containing duplexes. Additional studies are needed to explain the observed
16 sequence specific binding of other dsRNA binding proteins [5, 36, 49], and to understand
17 dsRBD binding to dsRNA with mismatches, small bulges and loops, common in microRNA
18 (miRNA) in the silencing by RNA interference pathways [15, 16].

19
20
21 **Acknowledgments.** This work was supported by the National Science Foundation (grant
22 NSF-PHY-0822613) and National Institutes of Health (grant NIH 9P41GM104601). We
23 acknowledge computer time provided by the Texas Advanced Computing Center (XSEDE
24 allocation MCB130078 to S. M.) and by the Computational Science and Engineering Pro-
25 gram at the University of Illinois (Taub computing cluster). L.V. acknowledges support as
26 a Center for the Physics of Living Cells (CPLC) Postdoctoral Fellow.

27
28
29 **Associated Content.** EMSA of 25-bp duplexes incubated with 0, 1, and $5 \mu\text{M}$ of TRBP-
30 RBD2. Number of hydrogen bonds between TRBP-RBD2 and the studied duplexes. A
31 table of averages for selected helical parameters. Time dependence of distances between
32 the positively charged TRBP-RBD2 residues and phosphate groups of the studied duplexes.
33 Snapshots of TRBP-RBD2 Lys210 and Lys214 fitting into the major grooves of the studied
34 duplexes. Duplex forms of dsRNA, DNA-RNA and dsDNA. Duplex forms at TRBP-RBD2
35 binding sites for the studied duplexes. Dihedral δ and phase angle P for DNA nucleotides of
36 DNA-RNA duplex. Contact area and interaction energy between TRBP-RBD1 and dsRNA.
37 This material is available free of charge via the Internet at <http://pubs.acs.org>

- [1] Carpenter, S., Aiello, D., Atianand, M. K., Ricci, E. P., Gandhi, P., Hall, L. L., Byron, M., Monks, B., Henry-Bezy, M., Lawrence, J. B., O'Neill, L. A. J., Moore, M. J., Caffrey, D. R., and Fitzgerald, K. A. (2013) A long noncoding RNA mediates both activation and repression of immune response genes. *Science* *341*, 789–792.
- [2] Hansen, T. B., Jensen, T. I., Clausen, B. H., Bramsen, J. B., Finsen, B., Damgaard, C. K., and Kjems, J. (2013) Natural RNA circles function as efficient microRNA sponges. *Nature* *495*, 384–388.
- [3] Han, B.-W. and Chen, Y.-Q. (2013) Potential pathological and functional links between long noncoding RNAs and hematopoiesis. *Sci. Signal.* *6*, 5.
- [4] Bartel, D. P. (2009) MicroRNAs: Target recognition and regulatory functions. *Cell* *136*, 215–233.
- [5] Masliah, G., Barraud, P., and Allain, F. H.-T. (2012) RNA recognition by double-stranded RNA binding domains: a matter of shape and sequence. *Cell. Mol. Life Sci.* *70*, 1875–1895.
- [6] Tian, B., Bevilacqua, P. C., Diegelman-Parente, A., and Mathews, M. B. (2004) The double-stranded-RNA-binding motif: interference and much more. *Nat. Rev. Mol. Cell Biol.* *5*, 1013–1023.
- [7] Saunders, L. R. and Barber, G. N. (2003) The dsRNA binding protein family: critical roles, diverse cellular functions. *FASEB J.* *17*, 961–983.
- [8] Nanduri, S., Carpick, B. W., Yang, Y., Williams, B. R., and Qin, J. (1998) Structure of the double-stranded RNA-binding domain of the protein kinase PKR reveals the molecular basis of its dsRNA-mediated activation. *EMBO J.* *17*, 5458–5465.
- [9] Lee, C.-G. and Hurwitz, J. (1992) A new RNA helicase isolated from HeLa cells that catalytically translocates in the 3' to 5' direction. *J. Biol. Chem.* *267*, 4398–4407.
- [10] Zhang, H., Kolb, F. A., Brondani, V., Billy, E., and Filipowicz, W. (2002) Human Dicer preferentially cleaves dsRNAs at their termini without a requirement for ATP. *EMBO J.* *21*, 5875–5885.
- [11] Wostenberg, C., Lary, J. W., Sahu, D., Acevedo, R., Quarles, K. A., Cole, J. L., and Showalter, S. A. (2012) The role of human Dicer-dsRBD in processing small regulatory RNAs. *PLoS ONE* *7*, e51829.

- 1
2
3
4
5
6
7
8
9
10
11
12
13
14
15
16
17
18
19
20
21
22
23
24
25
26
27
28
29
30
31
32
33
34
35
36
37
38
39
40
41
42
43
44
45
46
47
48
49
50
51
52
53
54
55
56
57
58
59
60
- [12] Knight, S. W. and Bass, B. L. (2002) The role of RNA editing by ADARs in RNAi. *Mol. Cell* 10, 809–817.
- [13] Daniels, S. M. and Gatignol, A. (2012) The multiple functions of TRBP, at the hub of cell responses to viruses, stress, and cancer. *Microbiol. Mol. Biol. R.* 76, 652–666.
- [14] Kok, K. H., Ng, M.-H. J., Ching, Y.-P., and Jin, D.-Y. (2007) Human TRBP and PACT directly interact with each other and associate with Dicer to facilitate the production of small interfering RNA. *J. Biol. Chem.* 282, 17649–17657.
- [15] Noland, C. L. and Doudna, J. A. (2013) Multiple sensors ensure guide strand selection in human RNAi pathways. *RNA* 5, 639–648.
- [16] Lee, H. Y., Zhou, K., Smith, A. M., Noland, C. L., and Doudna, J. A. (2013) Differential roles of human Dicer-binding proteins TRBP and PACT in small RNA processing. *Nucleic Acids Res.* 41, 6568–6576.
- [17] Wilson, R. C. and Doudna, J. A. (2013) Molecular mechanisms of RNA interference. *Annu. Rev. Biophys.* 42, 217–239.
- [18] Taylor, D. W., Ma, E., Shigematsu, H., Cianfrocco, M. A., Noland, C. L., Nagayama, K., Nogales, E., Doudna, J. A., and Wang, H.-W. (2013) Substrate-specific structural rearrangements of human Dicer. *Nat. Struc. Mol. Biol.* 20, 662–670.
- [19] Koh, H. R., Kidwell, M. A., Ragnathan, K., Doudna, J. A., and Myong, S. (2013) ATP-independent diffusion of double-stranded RNA binding proteins. *Proc. Natl. Acad. Sci. USA* 110, 151–156.
- [20] Gredell, J. A., Dittmer, M. J., Wu, M., Chan, C., and P., W. S. (2010) Recognition of siRNA asymmetry by TAR RNA binding protein. *Biochemistry* 49, 3148–3155.
- [21] Bevilacqua, P. C. and Cech, T. R. (1996) Minor-groove recognition of double-stranded RNA by the double-stranded RNA-binding domain from the RNA-activated protein kinase PKR. *Biochemistry* 35, 9983–9994.
- [22] Bass, B. L., Hurst, S. R., and Singer, J. D. (1994) Binding properties of newly identified *Xenopus* proteins containing dsRNA-binding motifs. *Curr. Biol.* 4, 301–314.
- [23] Castrignano, T., Chillemi, G., Varani, G., and Desideri, A. (2002) Molecular dynamics simulation of the RNA complex of a double-stranded RNA-binding domain reveals dynamic features of the intermolecular interface and its hydration. *Biophys. J.* 83, 3542–3552.
- [24] Yang, S. W., Chen, H.-Y., Yang, J., Machida, S., Chua, N.-H., and Yuan, Y. A. (2010)

- 1 Structure of Arabidopsis HYPONASTIC LEAVES1 and its molecular implications for miRNA
2 processing. *Structure* 18, 594–605.
- 3
4
- 5 [25] Lu, X.-J. and Olson, W. K. (2003) 3DNA: A software package for the analysis, rebuilding and
6 visualization of three-dimensional nucleic acid structures. *Nucleic Acids Res.* 31, 5108–5121.
- 7
8
- 9 [26] Humphrey, W., Dalke, A., and Schulten, K. (1996) VMD: Visual molecular dynamics. *J. Mol.*
10 *Graph.* 14, 33–38.
- 11
12
- 13 [27] Phillips, J. C., Braun, R., Wang, W., Gumbart, J., Tajkhorshid, E., Villa, E., Chipot, C.,
14 Skeel, R. D., Kalé, L., and Schulten, K. (2005) Scalable molecular dynamics with NAMD. *J.*
15 *Comput. Chem.* 26, 1781–1802.
- 16
17
- 18 [28] Hornak, V., Abel, R., Okur, A., Strockbine, B., Roitberg, A., and Simmerling, C. (2006)
19 Comparison of multiple Amber force fields and development of improved protein backbone
20 parameters. *Proteins* 65, 712–725.
- 21
22
- 23 [29] Perez, A., Marchan, I., Svozil, D., Sponer, J., Cheatham III, T. E., Laughton, C. A., and
24 Orozco, M. (2007) Refinement of the AMBER force field for nucleic acids: Improving the
25 description of α/γ conformers. *Biophys. J.* 92, 3817–3829.
- 26
27
- 28 [30] Besseova, I., Otyepka, M., Reblova, K., and Sponer, J. (2009) Dependence of A-RNA sim-
29 ulations on the choice of the force field and salt strength. *Phys. Chem. Chem. Phys.* 11,
30 10701–10711.
- 31
32
- 33 [31] Jung, S. and Schlick, T. (2014) Interconversion between parallel and antiparallel conformations
34 of a 4H RNA junction in domain 3 of foot-and-mouth disease virus IRES captured by dynamics
35 simulations. *Biophys. J.* 106, 447–458.
- 36
37
- 38 [32] Darden, T., York, D., and Pedersen, L. (1993) Particle mesh ewald: An $N \cdot \log(N)$ method
39 for Ewald sums in large systems. *J. Chem. Phys.* 98, 10089–10092.
- 40
41
- 42 [33] Parker, G. S., Maity, T. S., and Bass, B. L. (2008) dsRNA binding properties of RDE-4 and
43 TRBP reflect their distinct roles in RNAi. *J. Mol. Biol.* 384, 967–979.
- 44
45
- 46 [34] Ryter, J. M. and Schultz, S. C. (1998) Molecular basis of double-stranded RNA-protein
47 interactions: structure of a dsRNA-binding domain complexed with dsRNA. *EMBO J.* 17,
48 7505–7513.
- 49
50
- 51 [35] Gan, J., Shaw, G., Tropea, J. E., Waugh, D. S., Court, D. L., and Ji, X. (2008) A stepwise
52 model for double-stranded RNA processing by ribonuclease III. *Mol. Microbiol.* 67, 143–154.
- 53
54
- 55 [36] Stefl, R., Oberstrass, F. C., Hood, J. L., Jourdan, M., Zimmermann, M., Skrisovska, L., Maris,
- 56
57
58
59
60

- 1 C., Peng, L., Hofr, C., Emeson, R. B., and Allain, F. H.-T. (2010) The solution structure of
2 the ADAR2 dsRBM-RNA complex reveals a sequence-specific readout of the minor groove.
3 *Cell* 143, 225–237.
- 4
5
6
7 [37] Huang, Y., Ji, L., Huang, Q., Vassylyev, D. G., Chen, X., and Ma, J.-B. (2009) Structural
8 insights into mechanisms of the small RNA methyltransferase HEN1. *Nature* 461, 823–827.
- 9
10 [38] Lavery, R., Zakrzewska, K., Beveridge, D., Bishop, T. C., Case, D. A., Cheatham, T., Dixit,
11 S., Jayaram, B., Lankas, F., Laughton, C., Maddocks, J. H., Michon, A., Osman, R., Orozco,
12 M., Perez, A., Singh, T., Spackova, N., and Sponer, J. (2010) A systematic molecular dynamics
13 study of nearest-neighbor effects on base pair and base pair step conformations and fluctuations
14 in B-DNA. *Nucleic Acids Res.* 38, 299–313.
- 15
16
17 [39] Cheatham, T. E. and Kollman, P. A. (1997) Molecular dynamics simulations highlight the
18 structural differences among DNA:DNA, RNA:RNA, and DNA:RNA hybrid duplexes. *J. Am.*
19 *Chem. Soc.* 119, 4805–4825.
- 20
21
22 [40] Noy, A., Pérez, A., Máquez, M., Luque, F. J., and Orozco, M. (2005) Structure, recognition
23 properties, and flexibility of the DNA-RNA hybrid. *J. Am. Chem. Soc.* 127, 4910–4920.
- 24
25
26 [41] Dans, P. D., Pérez, A., Faustino, I., Lavery, R., and Orozco, M. (2012) Exploring polymor-
27 phisms in B-DNA helical conformations. *Nucleic Acids Res.* 40, 10668–10678.
- 28
29
30 [42] Yamashita, S., Nagata, T., Kawazoe, M., Takemoto, C., Kigawa, T., Gntert, P., Kobayashi,
31 N., Terada, T., Shirouzu, M., Wakiyama, M., Muto, Y., and Yokoyama, S. (2011) Structures
32 of the first and second double-stranded RNA-binding domains of human TAR RNA-binding
33 protein. *Prot. Sci.* 20, 118–130.
- 34
35
36 [43] Clemens, K., Wolf, V., McBryant, S., Zhang, P., Liao, X., Wright, P., and Gottesfeld, J.
37 (1993) Molecular basis for specific recognition of both RNA and DNA by a zinc finger protein.
38 *Science* 260, 530–533.
- 39
40
41 [44] Bycroft, M., Hubbard, T. J., Proctor, M., Freund, S. M., and Murzin, A. G. (1997) The
42 solution structure of the S1 RNA binding domain: A member of an ancient nucleic acid-
43 binding fold. *Cell* 88, 235–242.
- 44
45
46 [45] Barbas, A., Matos, R. G., Amblar, M., Lopez-Vinas, E., Gomez-Puertas, P., and Arraiano,
47 C. M. (2009) Determination of key residues for catalysis and RNA cleavage specificity: One
48 mutation turns RNase II into a “super-enzyme”. *J. Biol.Chem.* 284, 20486–20498.
- 49
50
51 [46] Jung, S.-R., Kim, E., Hwang, W., Shin, S., Song, J.-J., and Hohng, S. (2013) Dynamic
52
53
54
55
56
57
58
59
60

- 1 anchoring of the 3'-end of the guide strand controls the target dissociation of Argonaute-guide
2 complex. *J. Am. Chem. Soc.* *135*, 16865–16871.
- 3
4
5 [47] Pérez, A., Noy, A., Lankas, F., Luque, F. J., and Orozco, M. (2004) The relative flexibility of
6 B-DNA and A-RNA duplexes: database analysis. *Nucleic Acids Research* *32*, 6144–6151.
- 7
8
9 [48] McMillan, N. A. J., Carpick, B. W., Hollis, B., Toone, W. M., Zamanian-Daryoush, M., and
10 Williams, B. R. G. (1995) Mutational analysis of the double-stranded RNA (dsRNA) binding
11 domain of the dsRNA-activated protein kinase, PKR. *J. Biol. Chem.* *270*, 2601–2606.
- 12
13
14 [49] Eggington, J. M., Greene, T., and Bass, B. L. (2011) Predicting sites of ADAR editing in
15 double-stranded RNA. *Nat. Commun.* *2*, 319–1–9.
- 16
17
18
19
20
21
22
23
24
25
26
27
28
29
30
31
32
33
34
35
36
37
38
39
40
41
42
43
44
45
46
47
48
49
50
51
52
53
54
55
56
57
58
59
60

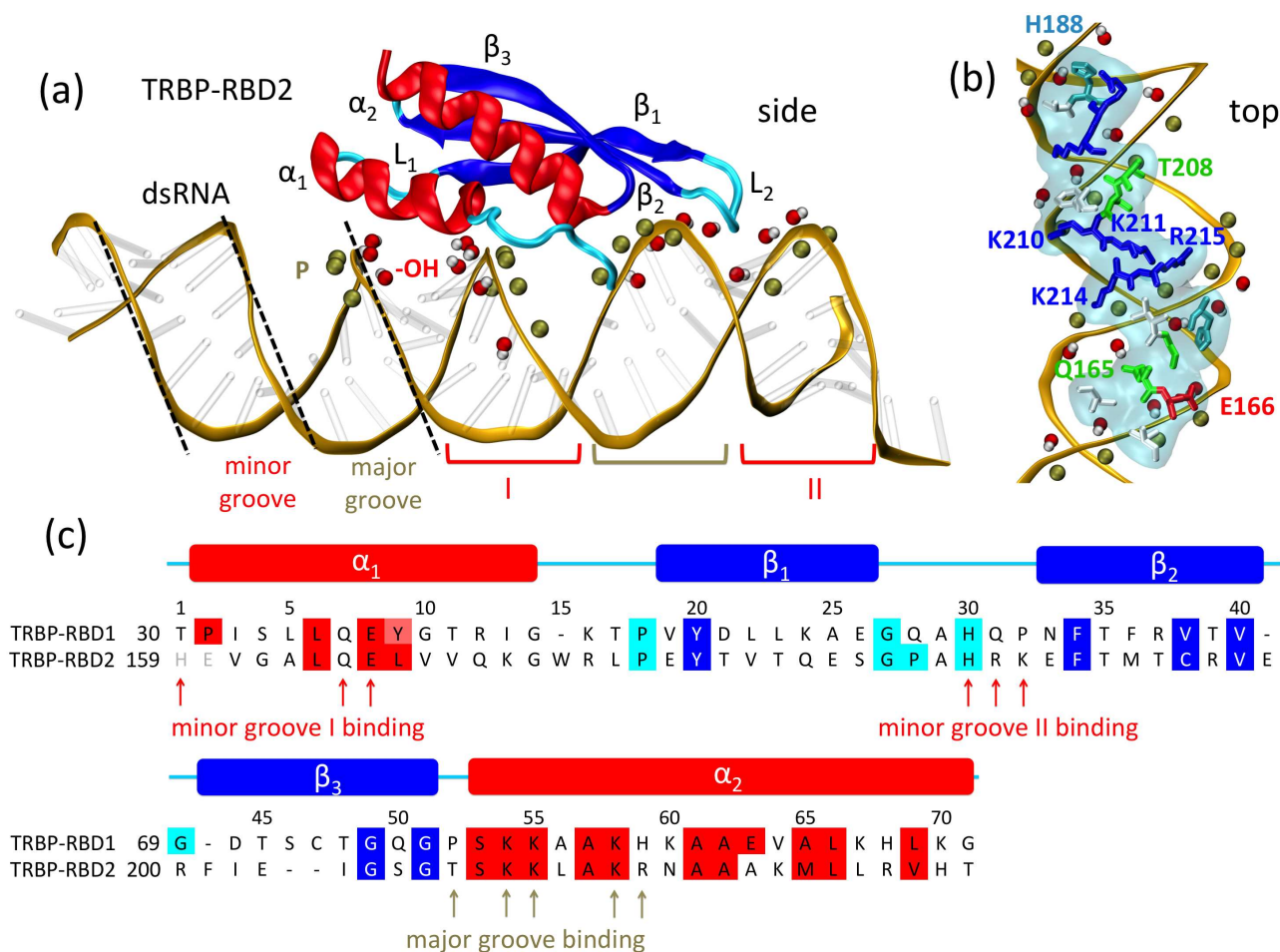


FIG. 1: Binding of TRBP-RBD2 to dsRNA. (a) Snapshot of the TRBP-RBD2:dsRNA complex. TRBP-RBD2 binds to dsRNA across three grooves, in minor-major-minor groove pattern. dsRNA minor grooves are lined with 2' hydroxyl groups (for clarity, only shown at the binding interface as red and white spheres), and its major grooves are lined with phosphate groups (P-atoms are shown as tan spheres). Minor and major grooves, which interact with TRBP-RBD2, are marked with red and tan brackets, respectively, the two minor grooves being distinguished by labels I and II. The RNA backbone is shown in gold, the bases are shown as transparent sticks, and TRBP-RBD2 is colored according to its secondary structure, where helices are shown in red, β -sheets in blue, and unstructured loops in cyan. (b) Top view of the binding interface of the TRBP-RBD2 : dsRNA complex. TRBP-RBD2 residues within 3 Å of the dsRNA are shown both as a transparent surface and in licorice representation. Blue residues are positively charged, red residues are negatively charged, green and cyan residues are polar, and white residues are nonpolar. (c) Sequence alignment of two TRBP dsRBDs. The residues conserved across different species and proteins are highlighted (Fig. S1 and [5]), where the colors indicate secondary structure elements, as shown in (a). The arrows point to TRBP-RBD2 residues that contact dsRNA; red and tan arrows mark minor and major groove contacts, respectively.

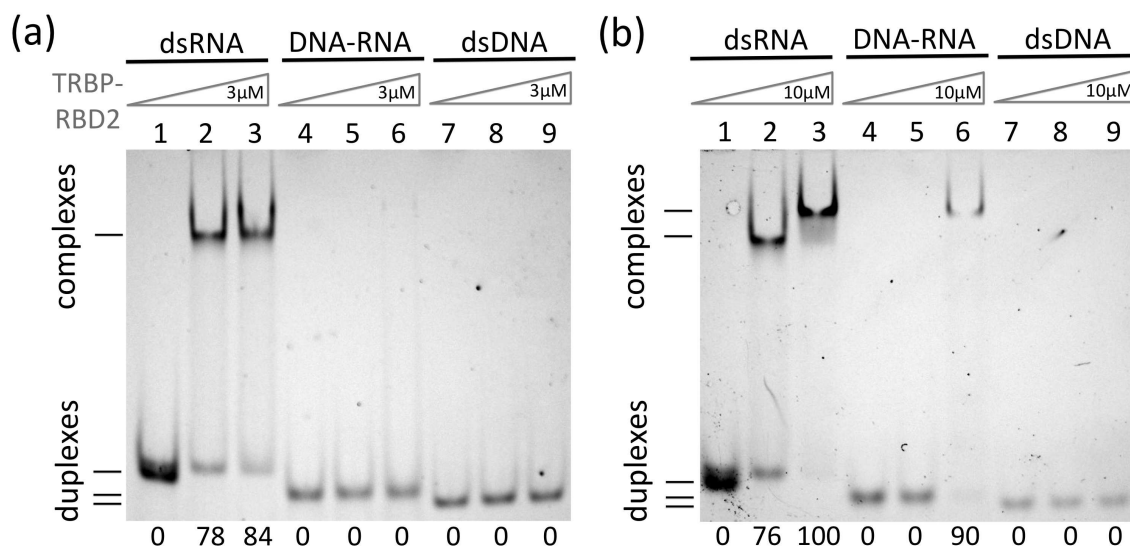


FIG. 2: EMSA demonstrates that the binding affinity of TRBP-RBD2 is strongest for dsRNA, and weakest for dsDNA. (a) EMSA of 25-bp duplexes incubated with 0, 1, and 3 μM of TRBP-RBD2. TRBP-RBD2 binds to dsRNA, and does not bind to DNA-RNA or dsDNA. (b) EMSA of 25-bp duplexes incubated with 0, 1, and 10 μM of TRBP-RBD2. TRBP binds to dsRNA and DNA:RNA (5-10 μM TRBP-RBD2, as shown in Fig. S2), and does not bind to dsDNA. The quantified binding fraction of TRBP-RBD2 to each duplex is displayed below the gel images.

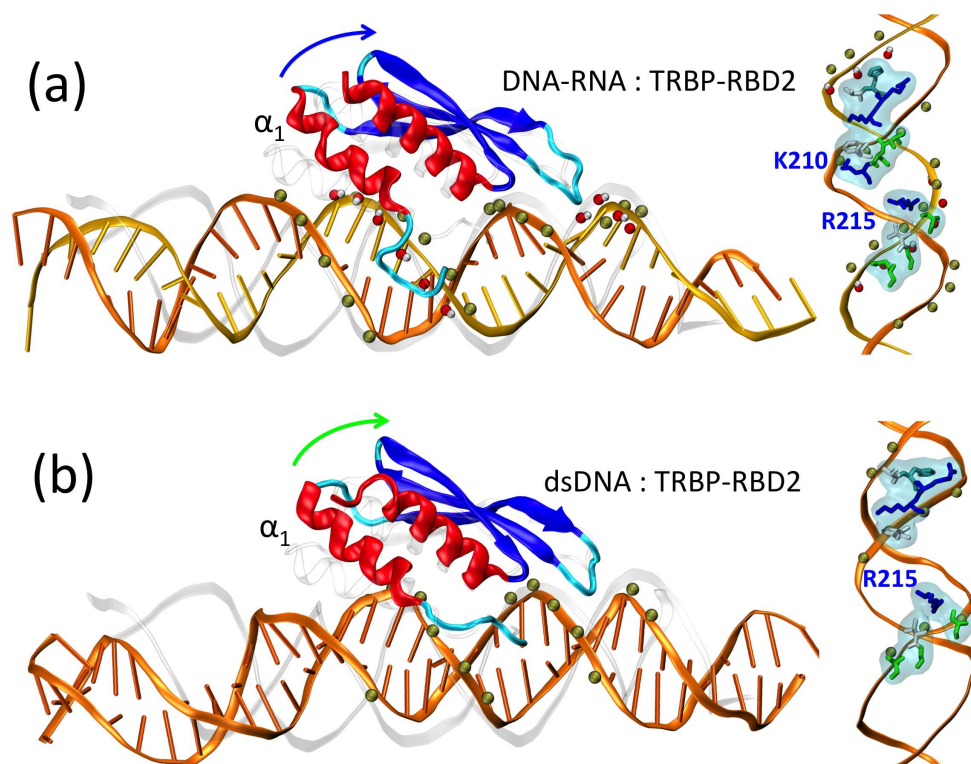


FIG. 3: Binding of TRBP-RBD2 to non-cognate duplexes: (a) DNA-RNA hybrid and (b) dsDNA. RNA strands are shown in gold color and DNA strands in orange. For comparison, the TRBP-RBD2 : dsRNA complex is shown in transparent ribbon representation with protein and RNA backbones aligned to the backbones of the complexes shown in color. Curved arrows mark displacements of α_1 helices of TRBP-RBD2 in complexes with DNA-RNA and dsDNA, as compared to complexes with dsRNA. Top views of binding interfaces are shown on the right, where TRBP-RBD2 residues within 3 Å of duplexes are highlighted in both transparent surface and licorice representations. The residues are colored according to residue type, as described in Fig. 1(b).

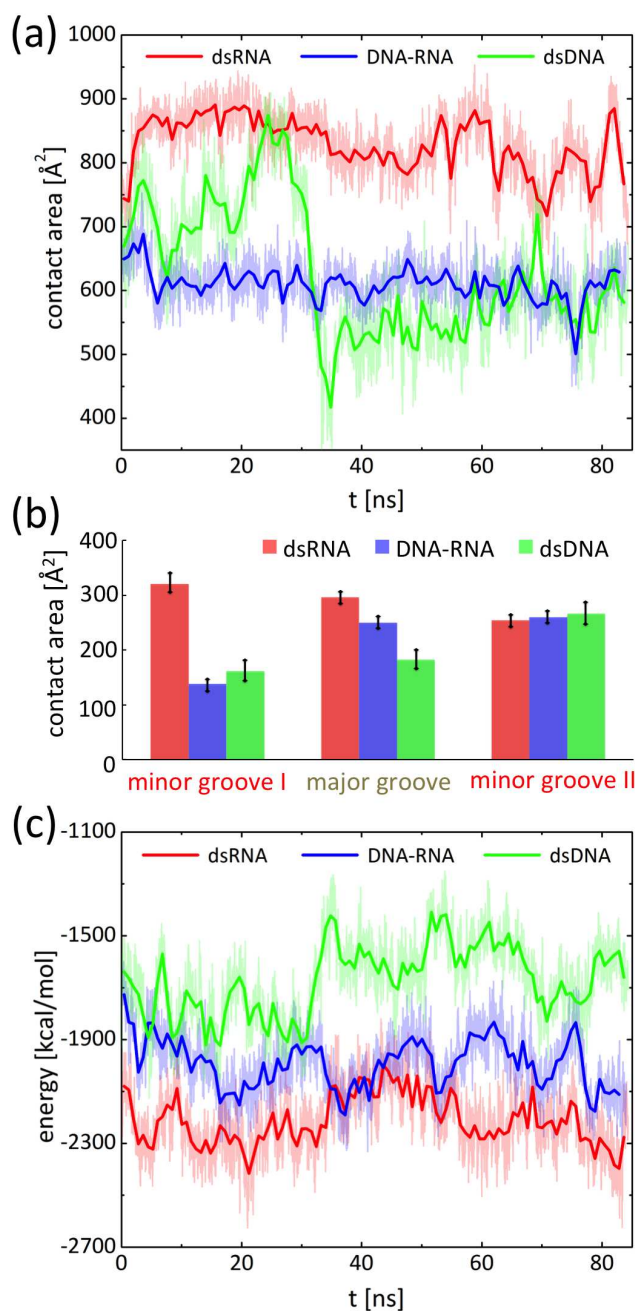


FIG. 4: Interaction of TRBP-RBD2 with three duplex types. (a) Contact areas between TRBP-RBD2 and dsRNA, DNA-RNA and dsDNA. (b) Contact areas between TRBP-RBD2 and individual nucleic acid grooves (minor grooves I and II, major groove, marked in Fig. 1 (a)). Contact areas were measured between whole duplexes and sets of the TRBP-RBD2 residues above the selected grooves, H159, E160, V161, G162, A163, Q165, E166, V168, V169, Q170, R174, L175, Y178 (for minor groove I); F192, T208, S209, K210, K211, L212, K214, R215 (major groove); E183, P186, A187, H188, R189, K190, E191 (minor groove II). (c) Interaction (nonbonding) energy between TRBP-RBD2 and the three duplexes. The plots are shown for the last 85 ns of trajectories. In (a), (c) thin lines correspond to data sampled from trajectories; thick lines show gliding time averages over 800 ps.

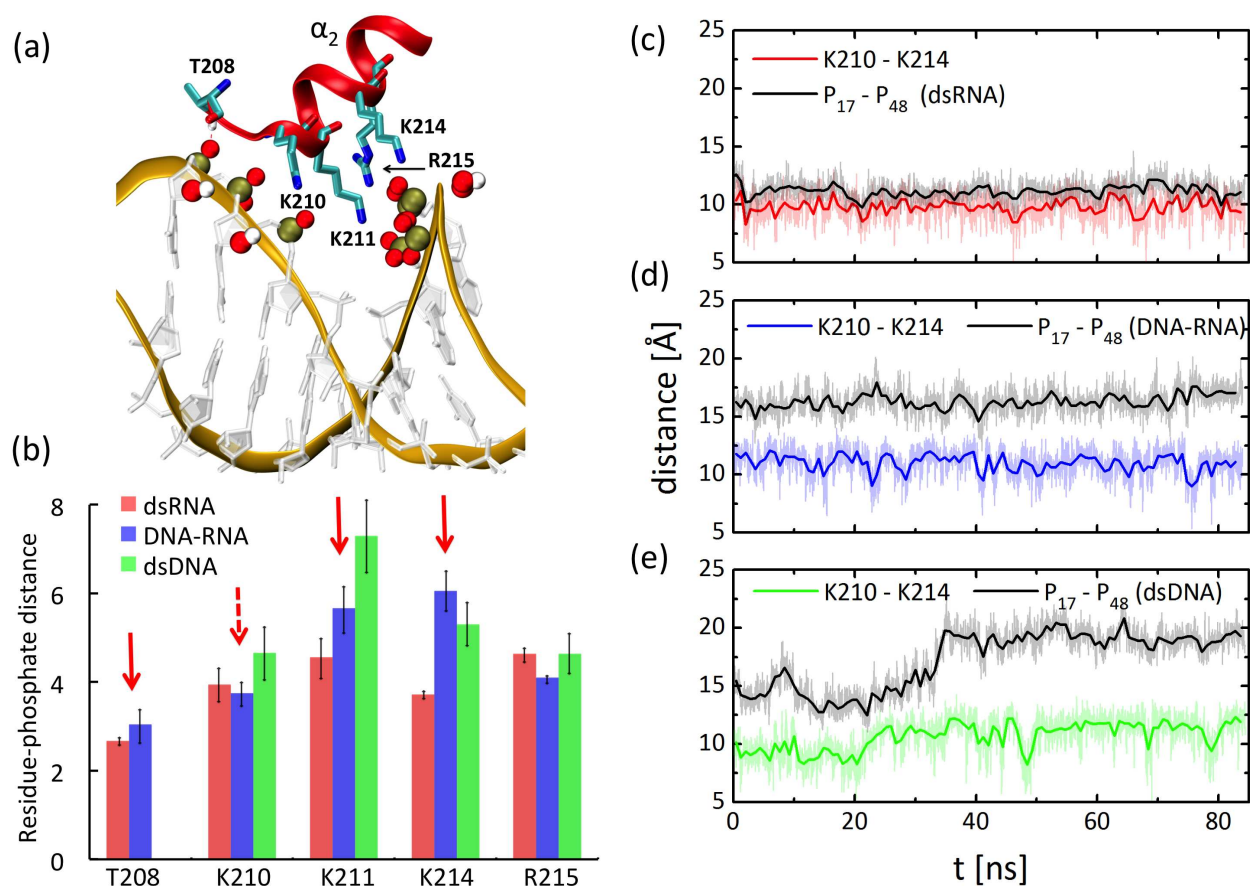


FIG. 5: Major groove interactions. (a) Binding of TRBP-RBD2 to the major groove of dsRNA. The residues which interact through Coulomb interactions (Lys and Arg) and hydrogen bonding (Thr) are highlighted, together with their bonding partners, negatively charged phosphate groups. Oxygen, hydrogen, and phosphorus atoms are shown as red, white, and tan spheres, respectively, carbon and nitrogen are shown in cyan and blue. (b) Average distances of TRBP-RBD2 residues from the phosphate groups nearest to them (phosphorus atoms for Lys and Arg, and oxygen atom for Thr208), averaged over the last 80 ns of simulations. Red arrows mark the residues which bind to dsRNA more tightly than to DNA-RNA or dsDNA. Register fit of Lys210-Lys214 pair in major grooves of dsRNA (c), DNA-RNA (d), dsDNA (e). Lys210-Lys214 distances and the distances between two phosphate groups that coordinate Lys210 and Lys214 are shown for three complexes. These distances are calculated between phosphate atoms of RNA nucleotides 17 and 48, and between nitrogen atoms of Lys210 and Lys214 sidechains. The distance between P₁₇ and P₄₈ characterizes the major groove width of the duplexes. In (c)-(e) thin lines correspond to data sampled from trajectories; thick lines show gliding time averages over 800 ps.

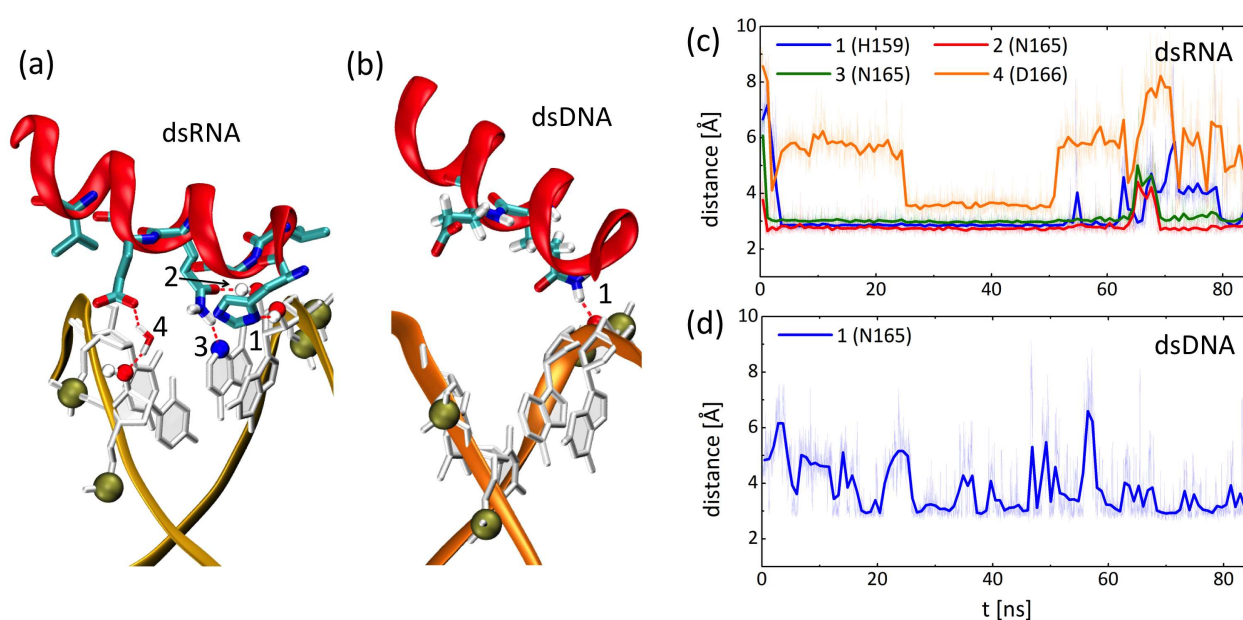


FIG. 6: Interactions of TRBP-RBD2 residues with minor grooves I of (a) dsRNA and (b) dsDNA. (c) Time dependent distances of stable contacts between TRBP-RBD2 and dsRNA minor groove I. (d) Same as in (c) for TRBP-RBD2 and dsDNA minor groove I. In (d) thin lines correspond to data sampled from trajectories; thick lines show gliding time averages over 800 ps.

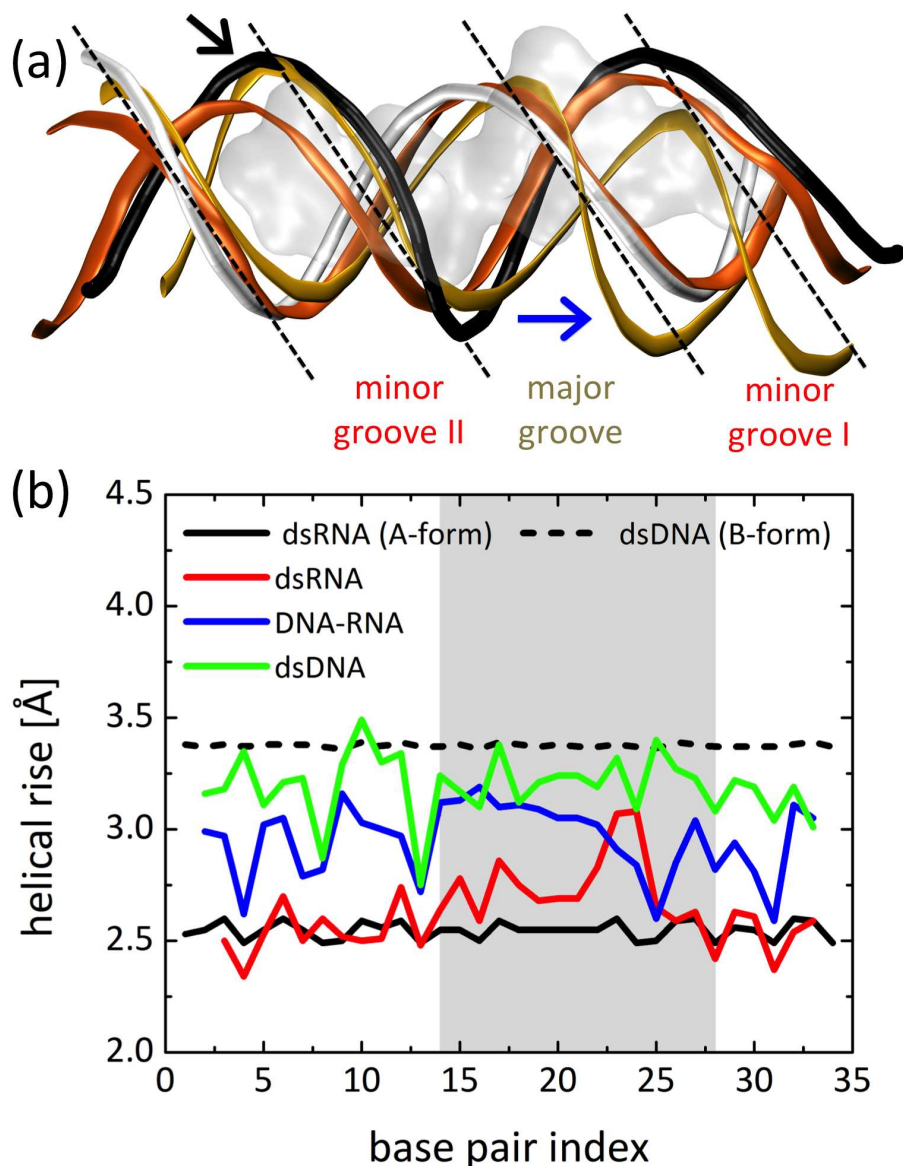


FIG. 7: Duplex forms at TRBP-RBD2 binding sites. The structures of complexes analyzed in (a-b) are obtained by averaging the coordinates of each system over the last 40 ns of simulation. (a) Duplex backbones at TRBP-RBD2 binding sites. dsRNA strands are shown in gold, dsDNA strands are shown in orange, and strands of the DNA-RNA hybrid are shown as black (DNA) and white (RNA) tubes. TRBP-RBD2 domains, bound to the shown duplexes, are aligned. The shaded area outlines the TRBP-RBD2 residues in contact with the dsRNA duplex (within 3.0 Å of it). The minor-major-minor groove pattern is labeled and highlighted by the black dashed lines. Black arrows point to major differences in duplex forms in binding regions. (b) Helical rise for duplex base pairs of A-form dsRNA, B-form dsDNA, and averaged structures of dsRNA, DNA-RNA, and dsDNA bound to TRBP-RBD2. The shaded region of the graph marks the base pairs which form the binding site for TRBP-RBD2. A- and B-form structures are generated with 3-DNA software [25].

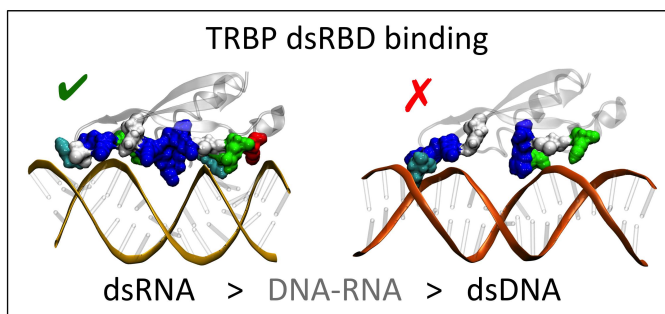


Table of Contents graphic